



Published in final edited form as:

J Am Chem Soc. 2019 February 13; 141(6): 2462–2473. doi:10.1021/jacs.8b12083.

A Click Chemistry Approach Reveals the Chromatin-Dependent Histone H3K36 Deacylase Nature of SIRT7

Wesley Wei Wang[†], Maria Angulo-Ibanez[‡], Jie Lyu[#], Yadagiri Kurra[†], Zhen Tong[¶], Bo Wu[†], Ling Zhang[§], Vangmayee Sharma[†], Jennifer Zhou[†], Hening Lin[¶], Yi Qin Gao[§], Wei Li[#], Katrin F. Chua^{‡, ⊥, *}, Wenshe Ray Liu^{†, *}

[†]Department of Chemistry, Texas A&M University, College Station, TX 77843, USA

[‡]Department of Medicine, Stanford University School of Medicine, Stanford, CA 94305, USA

[#]Division of Biostatistics, Dan L. Duncan Cancer Center, Baylor College of Medicine, Houston, Texas, USA

[¶]Howard Hughes Medical Institute, Department of Chemistry and Chemical Biology, Cornell University, Ithaca, NY 14853, USA

[§]Institute of Theoretical and Computational Chemistry, College of Chemistry and Molecular Engineering, Peking University, Beijing 100871, China

[⊥]Geriatric Research, Education, and Clinical Center, Veterans Affairs Palo Alto Health Care System, Palo Alto, CA 94304, USA

Abstract

Using an engineered pyrrolysyl-tRNA synthetase mutant together with tRNA_{CUA}^{Pyl}, we have genetically encoded *N*^ε-(7-azidoheptanoyl)-L-lysine (AzHeK) by amber codon in *Escherichia coli* for recombinant expression of a number of AzHeK-containing histone H3 proteins. We assembled *in vitro* acyl-nucleosomes from these recombinant acyl-H3 histones. All these acyl-nucleosomes contained an azide functionality that allowed quick click labeling with a strained alkyne dye for in-gel fluorescence analysis. Using these acyl-nucleosomes as substrates and click labeling as a detection method, we systematically investigated chromatin deacylation activities of SIRT7, a class III NAD⁺-dependent histone deacylase with roles in aging and cancer biology. Besides confirming the previously reported histone H3K18 deacylation activity, our results revealed that SIRT7 has an astonishingly high activity to catalyze deacylation of H3K36 and is also catalytically active to deacylate H3K37. We further demonstrated that this H3K36 deacylation activity is nucleosome dependent and can be significantly enhanced when appending the acyl-nucleosome substrate with a short double-stranded DNA that mimics the bridging DNA between nucleosomes in native chromatin. By overexpressing SIRT7 in human cells, we verified that SIRT7 natively

*Corresponding Author: wliu@chem.tamu.edu, kfchua@stanford.edu.

Supporting Information

The Supporting Information is available free of charge on the ACS Publications website.

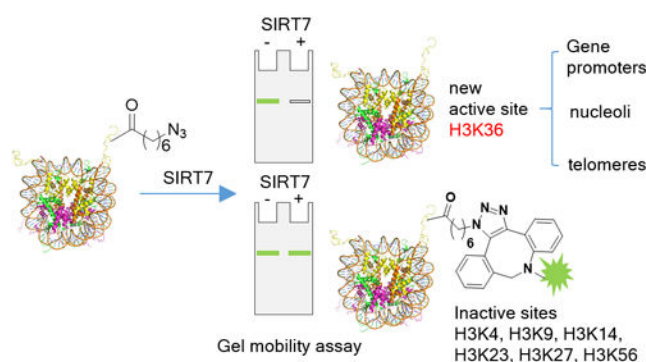
The synthesis of AzHeK and its characterization, experimental procedures of histone expression, nucleosome assembly, biochemistry assays, cell-based assays, and ChIP-seq analysis, and supplementary figures.

Notes

The authors declare no competing financial interest.

removes acetylation from histone H3K36. Moreover, SIRT7-deficient cells exhibited H3K36 hyperacetylation in whole cell extracts, at rDNA sequences in nucleoli, and at select SIRT7 target loci, demonstrating the physiologic importance of SIRT7 in determining endogenous H3K36 acetylation levels. H3K36 acetylation has been detected at active gene promoters, but little is understood about its regulation and functions. Our findings establish H3K36 as a physiologic substrate of SIRT7 and implicate this modification in potential SIRT7 pathways in heterochromatin silencing and genomic stability.

Graphical Abstract



INTRODUCTION

Sirtuins are class III histone deacetylases that rely on catalytic dissociation of nicotinamide from NAD⁺ to drive deacetylation from protein lysines.^{1–4} There exist seven sirtuins in humans, namely SIRT1–7.^{5,6} Four of these, SIRT1, 2, 6, and 7, can translocate to the nucleus, and therefore potentially remove acylation from chromatin for regulating chromatin epigenetic marks.^{3,7–9} Among these four sirtuins, SIRT7 is perhaps the least studied. Accumulating work suggests that SIRT7 has complex effects on cellular homeostasis, oncogenic potential, and cellular aging pathways.¹⁰ Multiple studies have observed high SIRT7 levels in cancers, including head and neck squamous cell carcinoma, colorectal cancer, early stage and metastatic breast cancer, thyroid carcinoma, ovarian cancer, and gastric cancer, consistent with oncogenic functions of SIRT7.^{11–20} Moreover, SIRT7 represses transcription of several tumor suppressive genes through deacetylation of histone H3 lysine 18 (H3 K18ac), and depletion of SIRT7 is sufficient to reduce malignant properties of cancer cells and inhibit tumor growth in mice.^{16,21} SIRT7 is enriched in nucleoli, and associates with both euchromatic and heterochromatic ribosomal DNA genes (rDNA).^{9,22,23} At euchromatic rDNA genes, SIRT7 deacetylates the RNA polymerase I (Pol I) subunit PAF53, which leads to enhanced interactions with rDNA for active transcription.^{9,24} This SIRT7-dependent rRNA synthesis may help support the high ribosome biogenesis, proliferative capacity, and metabolic demands of cancer cells.²⁵ However, SIRT7 also has tumor suppressive functions, and SIRT7-deficient mouse embryonic fibroblast cells show increased cell viability and cell-cycle entry into S and G2/M.^{26–29} Moreover, SIRT7 is recruited to DNA double-strand breaks (DSBs) and protects against DNA damage by promoting recruitment of 53BP1 for initiating Non-homologous End Joining.^{30,31} Recently, SIRT7 was also shown to guard against genomic instability due to rDNA rearrangements in

nucleoli, by maintaining rDNA heterochromatin silencing.²³ This function of SIRT7 is important for preventing senescence of human cells, which can contribute to tissue dysfunction in many aging-related pathologies and favor tumor growth in cancers. Thus, SIRT7 has pleiotropic effects on genomic stability and cellular homeostasis pathways that can impact on cancer and aging biology.

Although much evidence has established SIRT7 as a *bona fide* histone deacetylase, molecular details of SIRT7 interactions with chromatin for deacetylation have not been directly investigated. Two recent studies showed that both DNA and RNA can activate SIRT7.^{32,33} However, the mechanism of this activation process is yet to be illustrated. In the current study, we re-constituted *in vitro* acyl-nucleosomes that have acyl-lysines installed site-specifically at a number of native histone H3 lysine sites and used these recombinant acyl-nucleosomes as substrates to systematically investigate SIRT7 recognition of histone lysines for deacetylation in the physiologic context of chromatin. In addition to confirming the SIRT7 deacetylation activity on H3K18, we have uncovered two novel histone substrates of SIRT7, H3K36 and H3K37. Among these two, only acetylation at H3K36 has been validated as the physiological histone modification.^{34,35} We show that SIRT7 is a highly active, physiologic H3K36 deacetylase, and this activity is nucleosome or chromatin dependent and can be significantly enhanced when free DNA is appended to the acyl-nucleosome substrate. This novel activity of SIRT7 may serve a pivotal role in guarding against genomic instability and human cellular senescence in cancer and aging-related pathology.

RESULTS

SIRT7 is catalytically inert toward acetyl-histone H3 substrates.

In order to profile what histone H3 lysine sites are recognized by SIRT7 for acetylation removal, we initiated our study by testing SIRT7 activities on acetyl-H3 substrates that have been discovered in cells. We previously showed that histone H3 with acetyl-lysine (AcK) installed at K4, K9, K14, K18, K23, K27, K36, K56, and K79 positions can be recombinantly produced using the amber suppression-based genetic noncanonical amino acid (ncAA) mutagenesis approach.³⁶ In this recombinant expression technique, we used an acetyl-lysyl-tRNA synthetase (MmAcKRS1) that was evolved from *Methanosarcina mazei* pyrrolysyl-tRNA synthetase (MmPylRS1) and amber suppressing tRNA^{Pyl}_{CUA} to deliver AcK at an amber mutation site in a H3 mRNA during translation in *Escherichia coli*.^{37,38} MmAcKRS1, tRNA^{Pyl}_{CUA}, and H3 genes were all plasmid-born for transforming *E. coli* BL21(DE3) cells. We grew the transformed cells in the presence of AcK to produce acetyl-H3 proteins (H3K4ac, H3K9ac, H3K14ac, H3K18ac, H3K23ac, H3K27ac, H3K36ac, H3K56ac, and H3K79ac) that we purified and used as stand-alone substrates for SIRT1, 2, 6, and 7 during deacetylation assays. As a positive control, we carried out the same deacetylation assays of these acetyl-H3 substrates using a *Thermotoga maritima* sirtuin, Sir2Tm that has low substrate peptide sequence specificity. Our results revealed that Sir2Tm, SIRT1, and SIRT2 displayed strong deacetylation activities toward almost all acetyl-H3 substrates. We observed strong deacetylation of all acetyl-H3 substrates after their incubation with Sir2Tm, SIRT1, and SIRT2 and subsequent Western blotting with a pan

anti-Kac antibody. On the contrary, both SIRT6 and SIRT7 exhibited negligible activities toward all examined acetyl-H3 histone substrates (Figure S1). Previous studies showed that SIRT6 deacetylase activity requires nucleosomal substrates, and SIRT7-dependent H3K18 deacetylation was previously reported on nucleosomes.^{21,39} Since SIRT7 deacetylates histones in the setting of chromatin, we reasoned that its low activities towards all tested acetyl-H3 histone substrates might be due to the lack of nucleosomal chromatin context of the assay.

A click chemistry-based assay for quick profiling of SIRT7-targeted chromatin lysine deacylation sites.

Although originally defined as histone deacetylases, accumulated evidence has established that sirtuins catalyze the removal of a spectrum of acylation types from protein lysines.^{32,40–47} Therefore, they are categorized more generally as protein lysine deacylases. Specifically for SIRT7, studies have demonstrated that it catalytically removes fatty acyl and succinyl groups from histone lysines.^{32,47} Through genetic incorporation of *N*^ε-(7-octenoyl)-lysine (OcK) into histones in conjunction with the alkene-tetrazine cycloaddition reaction to analyze fatty acylation levels in acyl-nucleosome substrates that we assembled *in vitro* from OcK-incorporated histones, we previously revealed that SIRT6 is catalytically active to remove acylation from multiple H3 lysine sites.⁴⁸ Given the structural similarity between SIRT6 and SIRT7 and the demonstrated activity of SIRT7 to remove fatty-acylation from protein lysines, a similar approach might be applied to profile SIRT7-targeted H3 lysine deacylation sites. However, the previously described alkene-tetrazine cycloaddition-based method has a significant drawback. The slow reaction (the second order rate constant: $\sim 0.01 \text{ M}^{-1}\text{s}^{-1}$) between a terminal alkene and a tetrazine requires long reaction time.⁴⁹ Given the delicate nature of acyl-nucleosome substrates, this long reaction time is particularly undesirable. To accelerate the labeling reaction, we envisioned that *N*^ε-(7-azidoheptanoyl)-L-lysine (AzHeK) could be installed in acyl-nucleosome substrates and expected that AzHeK's close mimic of *N*^ε-decanoyl-L-lysine (DeK) would allow efficient recognition by SIRT7 for defatty-actylation. AzHeK has an azide functionality that reacts favorably with a dibenzocyclooctyne (DBCO) dye (the second order rate constant: $\sim 1 \text{ M}^{-1}\text{s}^{-1}$)^{50–52} for quick labeling of acyl-nucleosome substrates. Therefore, we can potentially use acyl-nucleosomes with AzHeK installed at different H3 lysine sites as SIRT7 substrates for defatty-acylation and then analyze relative activities of SIRT7 toward different acyl-nucleosomes by probing residual fatty-acylation on these substrates using a DBCO dye after their reactions with SIRT7 finish (Figure 1). Accordingly, an effective assay for profiling SIRT7 targeted H3 lysine deacylation sites can be potentially developed. This novel assay will allow not only straightforward determination of SIRT7 deacylation activities at different nucleosome lysine sites but also their quick kinetic characterization. In comparison to antibody-based detection, this designed assay is much simpler, quicker, and more accurate.

The genetic incorporation of AzHeK into a protein allows its click labeling with a strained alkyne dye.

Following a synthetic route shown in Scheme S1, we synthesized AzHeK in a gram quantity. For its genetic incorporation, we employed our previously identified OcKRS.⁴⁸ We have

shown that this MmPylRS mutant actively charges $\text{tRNA}_{\text{CUA}}^{\text{Pyl}}$ with OcK for their incorporation at amber codon during translation in *E. coli* (data not shown). When growing *E. coli* BL21(DE3) cells that harbored plasmids coding genes for OcKRS, $\text{tRNA}_{\text{CUA}}^{\text{Pyl}}$, and ubiquitin-6 \times His with an amber mutation at the K48 position in the presence of 1 mM AzHeK, we successfully induced the expression of full-length ubiquitin UbK48az (Figure 2B). The expression level was 18 mg/L, equivalent to the expression of Ub with OcK incorporated at K48. Wild type Ub has an expression level around 100 mg/L in the same conditions. On the contrary, we were not able to induce the expression of ubiquitin when AzHeK was absent. After incubating UbK48az with 100 μM MB488-DBCO, a strained alkyne dye for 1 h, we observed a strongly labeled ubiquitin band when we analyzed the protein using in-gel fluorescence (Figure 2C). However, the control wild-type ubiquitin was not labeled using the same conditions. In comparison to the previous alkene-tetrazine cycloaddition-based labeling that requires a minimum of 8 h for close to 40% labeling of an OcK-containing protein in the presence of a 200 μM tetrazine dye, this new labeling was much quicker and led to close to quantitative labeling in about 30 min (Figure S2). The azide group in UbK48az was stable at r. t. for about 1 h when 1 mM β -mercaptoethanol (BME) was present. We also characterized the purified UbK48az using MALDI-TOF mass spectrometry (Figure 2D). The MALDI-TOF-MS-determined molecular weight (9540.9 Da) agreed well with the calculated one (9540.7 Da).

SIRT7 catalyzes removal of acylation from H3 K18 and H3 K36 in the context of nucleosomes.

After confirming that OcKRS was efficient in mediating the genetic incorporation of AzHeK at amber codon, we proceeded to recombinantly express H3 proteins with AzHeK incorporated at K4, K9, K14, K18, K23, K27, K36, and K56, respectively. These AzHeK-containing H3 histones were named as H3K4az, H3K9az, and so on. To recombinantly produce a specific AzHeK-containing H3 protein, we transformed *E. coli* BL21(DE3) cells with pEVOL-OcKRS that contained genes coding OcKRS and $\text{tRNA}_{\text{CUA}}^{\text{Pyl}}$ and a pETDuet-H3 vector that contained a *N*-terminally 6 \times His-tagged H3 gene with an amber mutation introduced at a designated lysine coding site and grew the transformed cells in 2YT media supplemented with 1 mM AzHeK. We successfully expressed all eight proteins and affinity-purified them using Ni-NTA resins (Figure 3A). Expression levels of these proteins were much higher than their acetyl-H3 counterparts that typically required the supplementation of 2YT media with 5–10 mM AcK, potentially allowing easy and quick characterization of SIRT7-catalyzed deacylation of histones. Electrospray ionization mass spectrometry (ESI-MS) analysis of purified proteins confirmed the incorporation of AzHeK (Figures S3 and S4). Using these recombinantly produced acyl-H3 proteins together with H2A, H2B, H4, and 601 DNA,⁵³ we succeeded in reconstituting corresponding acyl-nucleosomes, named as nu-H3K4az, etc. that we visualized using ethidium bromide (EtBr) staining in a polyacrylamide gel (Figure 3B). We then subjected these *in vitro* assembled acyl-nucleosomes to deacylation by SIRT7. Acyl-nucleosomes treated with and without SIRT7 were then labeled with MB488-DBCO and imaged in 5% 1X TBE Native-PAGE gels. As shown in Figure 3C, SIRT7 removed acylation from H3K18 and H3K36 but was not active toward other lysine sites. The deacylation activity of SIRT7 on H3K36 is clearly much

higher than that on H3K18. The fluorescent gel showed total removal of acylation at H3K36 but residual acylation on H3 K18. H3 K18 was a previously demonstrated lysine deacylation site for SIRT7. However, SIRT7-catalyzed deacylation activity on H3K36 came as a surprise. We went further to quantify deacylation activities of SIRT7 on all tested sites. In the given deacylation conditions in which a 1 μM acyl-nucleosome was incubated with 0.5 μM SIRT7 and 1 mM NAD^+ at 37 $^\circ\text{C}$ for 2 h, the deacylation activity of SIRT7 on H3K36 was about 4 times of that on H3 K18 based on calculated deacylation percentages (Figure 3D).

DNA and salt inhibit SIRT7-catalyzed nucleosome deacylation.

Since a previous study reported that DNA activates SIRT7-catalyzed deacetylation on peptide substrates,³³ we investigated whether it has the same effect on SIRT7-catalyzed nucleosome deacylation. We used nu-H3K36az as a SIRT7 substrate and tested its deacylation by SIRT7 when we provided different concentrations of free 147 bp 601 DNA in the reaction solution. As shown in Figure 4A, SIRT7 strongly removed acylation from nu-H3K36az but this activity decreased significantly when we provided free DNA to the reaction solution and was close to be abolished when 2 μM free DNA was present. Thus, DNA apparently inhibits SIRT7-catalyzed nucleosome deacylation. Free DNA is negatively charged. It interacts electrostatically with both a positively charged histone-based peptide substrate and SIRT7 that has positively charged *N*- and *C*-termini. Therefore, it potentially serves as a bridge to bring SIRT7 and a peptide substrate in close proximity for improved deacetylation. We suspected that the wrapping DNA in an acyl-nucleosome substrate might play a similar role to interact electrostatically with SIRT7 for improved deacylation. To test this prospect, we examined SIRT7-catalyzed deacylation of nu-H3K36az in different concentrations of NaCl salt. If interactions between SIRT7 and nu-H3K36az are electrostatic in nature, increasing ionic strength of the reaction solution by providing NaCl will disrupt the binding of SIRT7 to nu-H3K36az and therefore leads to a lower deacylation activity. As expected, the SIRT7-catalyzed deacylation activity on the nu-H3K36az substrate diminished gradually when more salt was present in the reaction solution (Figure 4B). To confirm that free DNA does serve as a bridge to bring SIRT7 and a peptide or protein substrate into close proximity for improved deacylation activity, we tested the SIRT7-catalyzed deacylation activity on a soluble H3K36az-H4 tetramer substrate in the presence of various concentrations of free DNA. The result is shown in Figure 4C. Similar to its low activity toward H3K36ac, SIRT7 displayed a marginal deacylation activity on the H3K36az-H4 tetramer when free DNA was absent. However, this activity was significantly enhanced when we added 0.4 μM DNA into the reaction solution. When we added more DNA, this activity diminished gradually until it was almost totally abolished. This phenomenon is similar to what we observed with the nu-H3K36az substrate.

SIRT7 is more active toward acyl-nucleosomes with linker DNAs.

In chromatin, a bridging linker DNA that binds loosely to H1 and transcription factors connects two adjoining nucleosomes. To determine whether this linker DNA contributes to the binding of SIRT7 to an acyl-nucleosome for active deacylation, we synthesized nu-H3K18az and nu-H3K36az nucleosomes with different lengths of linker DNAs and used them as substrates to test SIRT7-catalyzed deacylation (Figures 5A & 5B). Appending a

linker DNA to nu-H3K36az significantly improved SIRT7-catalyzed deacylation (Figure 5C). A 5 bp linker DNA led to more than 3-fold increase of deacylation activity (Figure 5E). Increasing the linker DNA length from 5 bp to 20 bp slightly enhanced SIRT7 deacylation activity at H3 K36 but not to a significant level. Although appending the nu-H3K18az substrate with a linker DNA also improved SIRT7-catalyzed deacylation at H3 K18, this activity increase was much less significant than what we observed for the nu-H3K36ac substrate (Figures 5D & 5F). On the contrary, appending a linker DNA to nu-H3K4az, nu-H3K9az, nu-H3K14az, H3K23az, and H3K27az did not improve their deacylation by SIRT7 at all (Figure S5).

SIRT7 catalyzes removal of nucleosomal H3K36 acetylation *in vitro* and in cells.

Our finding that H3K36 is a preferential SIRT7-targeted lysine site for defatty-acylation led us to ask if SIRT7 is also catalytically active in removing acetylation at H3K36 both in *in vitro* biochemical assays and in cells. We assumed changing the modification type wouldn't change SIRT7 site-specificity, since the residues surrounding the modified lysine are the major contributing factors. We assembled two *in vitro* nu-H3K36ac nucleosomes using 147bp 601 DNA with or without a 20 bp linker DNA. We then incubated these two acetyl-nucleosomes with SIRT7 and subsequently detected acetylation levels of the reaction products by Western blotting with an anti-H3K36ac antibody. This analysis revealed that SIRT7 deacetylated H3K36 in the context of nucleosomes, and appending a linker DNA significantly improved this deacetylation activity (Figure 6A). To test SIRT7 activity on other nucleosomal H3 lysine sites, we also reconstituted several other acetyl-nucleosomes including nu-H3K4ac, nu-H3K9ac, nu-H3K14ac, nu-H3K18ac, nu-H3K23ac, nu-H3K27ac, and nu-H3K56ac (Figure S6) for use as substrates in SIRT7 deacetylation assays. All acetyl-nucleosomes contained a 20 bp linker DNA for improving SIRT7 activities. Our data confirmed that SIRT7 is also catalytically active to deacetylate H3K18 but inert toward all other tested lysine acetylation sites, and the deacetylation activity of SIRT7 on H3K18 is much weaker than that on H3K36. The relative deacetylation activity of SIRT7 on different H3 lysine sites matches exactly the relative deacylation activity on these sites that we obtained using AzHeK-containing nucleosomes as substrates. We also used nu-H3K36ac and nu-H3K18ac to carry out time-based deacetylation by SIRT7. Our determined results showed that AzHeK-containing nucleosomes mimic acetyl-nucleosomes in not only SIRT7-targeted lysine deacylation sites but also SIRT7-catalyzed deacylation activity (Figure S7). To examine the deacetylase activity of SIRT7 on H3K18 and H3K36 in cells, we constructed two plasmids, one coding a SIRT7-EGFP fusion gene and the other a SIRT7-EGFP fusion gene with a H187Y mutation to inactivate the SIRT7 activity, from a mammalian pEGFP vector. Together with the original pEGFP vector, we transiently transfected 293T cells separately with all three plasmids. We separated cell lysates from these three transiently transfected cells using SDS-PAGE and then analyzed different histone acetylation levels using antibodies that recognize acetylation at K9, K14, K23, K27, and K36 of H3, respectively. These assays revealed significantly decreased acetylation levels at H3K18 and H3K36 in cells with overexpressed SIRT7-EGFP but not in cells transfected with the empty control vector or expressing the inactive SIRT7-H187Y-EGFP fusion protein. These data demonstrate that SIRT7 is catalytically active in deacetylating both H3K18 and H3K36 in cells. Although our *in vitro* analysis indicates that SIRT7 is four-fold more active to

deacetylate H3K36 than H3K18, our cell based assay showed similar acetylation decrease at both sites when SIRT7 was transiently expressed (Figure S8). It is likely that numerous cellular factors influence the overall effects of SIRT7 over-expression on cellular H3K36 or H3K18ac levels, including SIRT7 regulatory factors, acetyltransferase enzymes, or compensatory deacetylase enzymes.

SIRT7 is essential for maintaining low H3K36ac levels at nucleolar rDNA sequences and select gene promoters.

We next asked if H3K36ac is a physiologic substrate of SIRT7, and if endogenous SIRT7 is important for setting baseline levels of H3K36 acetylation. We generated SIRT7-deficient cells by shRNA-mediated knockdown strategies, and assayed levels of H3K36ac in whole cell extracts by Western analysis (Figure 7A). We observed significantly increased H3K36 acetylation in the SIRT7-depleted cells. We also examined locus-specific H3K36ac levels at promoters of previously described genomic targets of SIRT7 by chromatin immunoprecipitation (ChIP).²¹ In SIRT7-depleted cells, levels of H3K36ac were significantly increased at two ribosomal protein gene targets of SIRT7, but not at another SIRT7 target, COPS2 (Figure 7B). SIRT7 is known to deacetylate H3K18ac at the RPS20 and COPS2 promoters²¹. Our data suggest that SIRT7 loss leads to increased acetylation of both H3K36 and H3K18 at the RPS20 promoter, but only affects H3K18 acetylation at the COPS2 promoter. These observations imply that the effects of SIRT7 on the two acetylation sites depends on other cellular factors. We also confirmed these findings using an independent H3K36ac antibody, since antibody reagents for H3K36ac ChIP have not been extensively characterized (Figure 7B). SIRT7 is reported to be enriched in nucleoli based on immunofluorescence studies. To examine changes in H3K36 acetylation specifically in nucleoli, we carried out biochemical fractionation of SIRT7-deficient and control cell extracts into nucleolar and nucleoplasmic (non-nucleolar) fractions. Immunoblot analysis revealed that both nucleolar and nucleoplasmic levels of H3K36ac are dramatically increased in SIRT7-depleted cells compared to control cells (Figure 7C). To further validate these findings in cells completely lacking SIRT7, we used CRISPR/Cas9 targeting to generate two independent SIRT7-knockout cell lines and a non-targeted control-treated cell line. Nucleolar fractionation of the cells confirmed the dramatic increase in H3K36ac levels in both nucleoli and nucleoplasm of SIRT7-knockout cells (Figure 7D). Importantly, in the control cells, H3K36ac levels (relative to total H3) were much lower in nucleoli than nucleoplasm, and this inversely correlated with SIRT7 levels in those nuclear compartments. This observation further underscores the physiological relevance of SIRT7 deacetylase activity in maintaining low H3K36ac levels in a non-perturbed system, particularly in nucleoli. The main DNA components of nucleoli are rDNA genes. To directly assess H3K36 acetylation changes at rDNA, we analyzed H3K36ac ChIPs from SIRT7-deficient and control cells using real-time PCR or unbiased high-throughput sequencing. The ChIP-PCR revealed significantly increased H3K36ac occupancy at rDNA sequences (Figure 7E). Notably, analysis of the high-throughput sequencing reads from the ChIPs confirmed these findings, and showed that the increase in H3K36ac is quite specific to rDNA compared to other repetitive regions of the genome, as no significant changes in acetylation were observed at repetitive sequence tracts present at over 20 different centromeric and pericentromeric regions, or when queried for eight different centromeric and pericentromeric

consensus repeat sequences (Figure 7F).⁵⁴ Finally, this analysis also revealed an intriguing and unexpected increase in H3K36ac occupancy at TTAGGG repeats, which are present at telomeres. Together, our studies demonstrate that SIRT7 is a novel physiologic H3K36 deacetylase, and is essential for maintaining low H3K36 acetylation levels at rDNA sequences in nucleoli, certain protein-coding genes, and possibly telomeric DNA.

H3K36 acylation leads to a loose nucleosome complex.

H3K36 is located at the entry and exit sites of DNA in the nucleosome dyad, according to the crystal structure information.⁵⁵ Its positively charged side chain amine can interact directly with a negatively charged DNA backbone phosphate. This potential electrostatic interaction is expected to contribute to a tightly bound nucleosome complex that prevents access to H3K36 by enzymes and transcription factors including SIRT7. The disruption of this electrostatic interaction by H3K36 acylation will weaken the binding of DNA to the nucleosome core, therefore leading to more frequent unwrapping of DNA from core histones and consequently more accessibility to enzymes and transcription factors. We think this potentially increased unwrapping of DNA from the nucleosome core assists SIRT7-catalyzed deacetylation at H3K36. This improved unwrapping of DNA from the nucleosome core will also lead to more access of DNA by a nuclease (Figure 8A). To test whether H3K36 acetylation improves DNA unwrapping, we introduced a Pst1 endonuclease restriction site at the entry/exit site of 601 DNA that also contained a 20 bp linker DNA beyond the Pst1 restriction site and used this mutant 601 DNA to reconstitute three nucleosomes including wild type (nu') with no histone modification, nu'-H3K18ac, and nu'-H3K36ac for analyzing effects of acetylation of H3 K18 and H3 K36 on Pst1-catalyzed restriction digestion of the wrapping DNA (Figure 8B and Figure S9). We introduced the Pst1-cutting site at the entry/exit site in order to maintain the nucleosome integrity after Pst1-catalyzed restriction cleavage of the tail linker DNA fragment. Since the digested nucleosome has a shorter DNA, it will run faster than the original nucleosome and can be easily visualized in a 5% 1× TBE native-PAGE gel after EtBr staining. We included nu'-H3K18ac in our analysis to see whether acetylation may generally increase DNA unwrapping from the nucleosome histone core. As shown in Figure 8C, Pst1 showed higher activities to digest DNA in nu'-H3K18ac and nu'-H3K36ac than DNA in nu' that had no histone lysine acetylation. The effect of H3K36 acetylation is much more significant than that of H3K18 acetylation (Figure 8D). The loose nucleosome conformation caused by H3K36ac could be an explanation why H3K36ac has correlated with activated gene transcription⁵⁶ and higher chromatin remodeling activity of chd1.⁵⁷ The H3K56 residue is located at a histone core region close to the DNA entry-exit site. Published crystal structures have shown that it interacts electrostatically and directly with the wrapping DNA.^{55,58} Its acetylation that neutralizes the side chain charge is expected to significantly weaken the DNA-core binding and therefore lead to an even more relaxed nucleosome conformation than H3K36ac. To confirm this aspect, we assembled nu'-H3K56ac and did a similar Pst1 digestion analysis. Our results showed that nu'-H3K56ac is more readily digested by Pst1 than nu'-H3K36ac (Figure 8D), confirming what we expected.

SIRT7 deacetylates H3K37 *in vitro*.

A recent report indicated that SIRT7 might also be catalytically active to deacetylate H3K37.⁵⁹ To test this aspect, we expressed H3K37ac and subsequently assembled nu-H3K37ac. Incubating nu-H3K37ac with SIRT7 followed by Western blotting clearly indicated that SIRT7 removed acetylation from H3K37 (Figure 9A). To compare the *in vitro* deacetylation activity of SIRT7 on the three currently known H3 lysine substrates of SIRT7, we analyzed time-based SIRT7-catalyzed deacetylation of nu-H3K18ac, nu-H3K36ac, and H3K37ac (Figures 9 B–D). Our data indicated that SIRT7's activity on nu-H3K37ac is significantly lower than that on nu-H3K36ac but higher than that on nu-H3K18ac. Notably, however, in SIRT7 knockout U2OS cell lines, H3K37ac levels were not significantly altered in comparison to control cells (Figure 9E). This observation indicates that SIRT7 does not have a physiologic role in maintaining global H3K37 deacetylation in cells. It is possible that SIRT7 does deacetylate H3K37 in yet-to-be identified physiologic or genomic settings, and this will be an interesting area of future research.

DISCUSSION

For kinetic analysis of histone modifying enzymes, peptide-based substrates are typically used, which accounts for straightforward characterization of both substrates and products using HPLC, mass spectrometry, and other methods. However, these analytical methods are difficult to apply to histone and nucleosome-based substrates. Although Western blot can serve as an alternative analytical approach, accurate quantification based on antibody detection is relatively difficult. Inspired by the finding that some sirtuins are general deacylases that catalytically remove a number of acylation types, we previously demonstrated that a long chain terminal olefin-containing fatty acylation on a nucleosomal lysine in combination with an olefin-tetrazine cycloaddition reaction to fluorescently label a fatty acyl-nucleosome allowed characterization of SIRT6-targeted histone deacetylation in the nucleosome context.⁴⁸ However, the reaction used in the SIRT6 study was kinetically slow, which required long labeling time. To resolve this problem, we demonstrated the genetic encoding of AzHeK in the current study for the synthesis of azide-containing fatty acyl-nucleosomes that can be quickly labeled with a DBCO-based dye but still serve as substrates for SIRT7. Using this new click chemistry-based approach, we expediently characterized SIRT7-catalyzed deacetylation on multiple acyl-nucleosome substrates. Given that SIRT1, SIRT2, SIRT6, and SIRT7 share similar catalytic features⁴⁰ and some Zn²⁺-dependent HDACs are also active to remove long chain fatty acylation from histone lysines,^{60,61} this newly developed method can potentially serve as an efficient tool to study all these enzymes.

SIRT7 is a demonstrated histone H3K18 deacetylase in cells. However, it doesn't display appreciable activity when assayed on H3K18ac as a free histone H3 protein. Our studies also showed no SIRT7 activity with 8 other acetyl-H3 histone substrates. Apparently, SIRT7 is inactive toward a stand-alone acetyl-histone substrate. SIRT7 has an isoelectric point (pI) as 9.8. This high pI makes it highly positively charged at physiological pH. The calculated positive net charges determined by Protein Calculator v3.4 at pH 7.4 for SIRT7 are about 24. Histone H3 naturally has many lysine and arginine residues, which result in also a high pI value as 11.1. At pH 7.4, an acetyl-H3 will have positive net charges about 19. Since both

SIRT7 and an acetyl-H3 substrate are highly positively charged at physiological pH, they will naturally have strong electrostatic repulsion that prevents their direct binding for deacetylation. This explains our *in vitro* data and also supports the notion that SIRT7 doesn't natively deacetylate free histones in cells. We have also made a similar observation with SIRT6, a close homolog of SIRT7. Although SIRT6 actively removes acetylation from H3K9 in cells,⁸ it is inactive toward an H3K9ac substrate *in vitro*. Like SIRT7, SIRT6 has a high pI value as 9.3 that makes it highly positively charged at physiological pH and consequently repels the binding of an acetyl-H3 substrate. Although SIRT6 and SIRT7 naturally repel acetyl-histone substrates, their highly positively charged nature makes them easily associate electrostatically with negatively charged DNA in chromatin, consistent with their reported functions as chromatin binding enzymes. In a chromatin setting, not only does chromosomal DNA neutralize positive charges in both SIRT6 or SIRT7 and an acetyl-histone substrate for relieving their electrostatic repulsion, but it also serves as a mediator to bring SIRT6 or SIRT7 and the acetyl-histone substrate into close proximity for deacetylation. As shown here for SIRT7 and previously for SIRT6, putting H3K18ac and H3K9ac in a nucleosome context significantly enhanced their deacetylation by SIRT7 and SIRT6, respectively. Therefore, both enzymes are nucleosome-dependent deacylases. DNA in chromatin also serves to activate SIRT7. A previous report showed that free DNA activates SIRT7-catalyzed deacetylation of an acetyl-peptide substrate.³³ We re-evaluated this potential DNA activating effect using both an acyl-nucleosome substrate and an acyl-H3-H4 tetramer substrate. Providing free DNA clearly inhibited SIRT7-catalyzed deacylation of the acyl-nucleosome substrate. However, adding a small amount of DNA to the acyl-H3/H4 tetramer substrate significantly improved its deacylation by SIRT7 at the beginning but this improvement was offset when additional DNA was added. These results support our conclusion that DNA serves only as a mediator to bring SIRT7 and an acyl-histone substrate into close proximity for deacylation. Free DNA competes against an acyl-nucleosome substrate for binding SIRT7 and therefore inhibits SIRT7-catalyzed deacylation of the acyl-nucleosome substrate. However, when DNA is provided in a small amount to an acyl-H3-H4 tetramer substrate, a single DNA fragment is able to bind both SIRT7 and the acyl-H3-H4 tetramer substrate to form a 1:1:1 complex and therefore serves to bring them to close proximity for interactions and deacylation. When provided in a large amount, additional DNA competes against the formation of a DNA-SIRT7-substrate (1:1:1) complex that is required for deacylation and consequently brings down the SIRT7-catalyzed deacylation of the acyl-H3-H4 tetramer substrate. The interactions between DNA and SIRT7 are largely electrostatic in nature. When we provided NaCl that disrupts electrostatic interactions, the activity of SIRT7 on an acyl-nucleosome substrate was clearly inhibited. We further confirmed the electrostatic nature of DNA-SIRT7 interactions by appending an acyl-nucleosome substrate with two additional linker DNAs to show an improved deacylation activity by SIRT7. These linker DNAs do not directly participate in the nucleosome complex formation. Their negative charges are less neutralized like the wrapping DNA. With more net negative charges, they were expected to interact more efficiently with SIRT7 than the wrapping DNA for improving SIRT7 binding and recognition of the integrated acyl-histone substrate in the nucleosome context for deacylation. This was exactly what our results showed.

Our current SIRT7 study also points out a critical aspect of epigenetic enzymes that might have been long ignored in their biochemical analysis. Most histone modifying enzymes naturally interact directly or indirectly with chromatin in which the nucleosome is the smallest subunit. It is logical to consider that corresponding nucleosome substrates might be minimally required to study these enzymes in a setting that properly recapitulates the physiologic context of their catalytic activity in cells. However, for convenience reasons, many biochemical studies of histone modifying enzymes have been based on peptide substrates or free histone proteins. How much the activity of a histone modifying enzyme on a peptide or histone substrate deviates from that on a nucleosome or chromatin substrate is a significant concern. Many histone modifying enzymes such as GCN5, MLL1–2, Suv39h1–2, Suv420h1–2, Dot1L, and KDM4D share highly basic features similar to SIRT6 and SIRT7. Thus, their strong interactions with chromatin for improved activities on histones are expected. There are also a large number of histone modifying enzymes that have strong acidic features. Most Zn²⁺-dependent HDACs have relatively low pI values. At physiological pH, they are highly negatively charged and thus expected to bind tightly to histones but resist the association with chromatin. Although peptide substrate-based data have indicated strong deacetylation activities for most Zn²⁺-dependent HDACs,⁶² it is doubtful that these enzymes behave the same on nucleosome or chromatin substrates. Many Zn²⁺-dependent HDACs are part of transcription factor complexes that associate with chromatin. It is highly possible they are brought into interactions with their histone substrates within chromatin by their associated partners in these complexes to avoid electrostatic repulsion with chromatin DNA. As shown in a recent study, an HDAC1 complex behaves very differently on peptides and nucleosome substrates.⁶³ Supported by the SIRT7 study in this work and our previous study with SIRT6, we strongly recommend re-characterizing biochemistry of most histone modifying enzymes using related nucleosome substrates.

As for SIRT7-targeted H3 lysine deacetylation sites, we have successfully confirmed the previously discovered H3 K18 site, but in addition, have uncovered H3K36 and H3K37 as surprising new substrate sites. Moreover, SIRT7 is several folds more active in deacetylating H3K36 than H3K18. We did not observe appreciable activities on other tested H3 lysine sites. H3K18 and H3K36 have both low peptide sequence resemblance and low chemical environment resemblance. How SIRT7 recognizes these two dissimilar lysine sites for deacylation is very intriguing. Interestingly, H3K18 highly resembles H3K9 and H3K27 in peptide sequence contexts. All three lysines are in the H3 *N*-terminal tail with much lower structural constraint in comparison to H3K36 that is at the DNA entry/exit site of the nucleosome dyad. Our previous study showed that SIRT6 was mainly active in deacetylating these three H3 lysine sites probably due to their consensual sequence contexts.⁴⁸ It is quite puzzling that SIRT7, a close homolog of SIRT6, deacylates H3K18 but is totally inert toward H3K9 and H3K27. Given that H3K36 is at the DNA entry/exit site of the nucleosome dyad, unwrapping DNA partially from the nucleosome core will be necessary to leave enough space for SIRT7 to bind and deacylate it. How SIRT7 unwraps DNA and then interacts with both DNA and H3K36 is perplexing. Before the structure of SIRT7 complexed with an acyl-nucleosome substrate is finally determined, we hesitate to postulate a theory to explain our observation.

H3K36ac is an active transcription mark that accumulates at transcription start sites.⁵⁶ It is enriched in euchromatin, which is possibly due to its potential weakening of the nucleosome complex.⁶⁴ Our *in vitro* assembled nu'-H3K36ac did show more DNA unwrapping than the nucleosome without any acetylation (Figure 8). When we overexpressed SIRT7 in cells, we observed down-regulation of acetylation at both H3K18 and H3K36, confirming H3K36 as a cellular deacetylation target of SIRT7. Importantly, we also showed that loss of SIRT7 in human cells leads to hyperacetylation of H3K36, which can be detected at the level of whole cell extracts, isolated nucleoli, and select SIRT7 target promoters. These findings demonstrate that endogenous SIRT7 has an essential function in determining the physiologic levels of this acetylation mark. A previous study revealed that providing nicotinamide, a sirtuin inhibitor, to cells leads to significant acetylation level increases at H3K36.⁶⁵ Our study implies that this effect is highly likely due to the inhibition of SIRT7.

Our biochemical fractionation and ChIP studies also reveal the pivotal role of SIRT7 in maintaining low H3K36ac levels at rDNA in nucleoli. SIRT7 has two distinct functions at rDNA sequences, which exist in either active or silent chromatin states. At active rDNA, where SIRT7 was previously linked to rDNA transcriptional activation, SIRT7-dependent removal of H3K36ac might allow for maintenance of H3K36me3, which is associated with transcription elongation.²² By contrast, at silent rDNA regions, H3K36 deacetylation by SIRT7 might have a novel function in contributing to SIRT7 effects on heterochromatin maintenance and prevention of rDNA instability.²³ Intriguingly, we also detected increased levels of TTAGGG repeats in the ChIP-seq reads from SIRT7-knockdown cells compared to controls, suggesting a potential function of SIRT7 deacetylase activity on H3K36 at telomeres. However, we have not previously detected SIRT7 at telomeres, and additional studies will be important to evaluate this possibility. Finally, SIRT7 is recruited to DNA DSBs where it contributes to DNA damage responses.³¹ An intriguing possibility is that SIRT7-dependent deacetylation of H3K36 at DSBs might clear the way for generation of H3K36me3, a critical mediator of DNA damage signaling.

CONCLUSION

In summary, we have genetically encoded AzHeK in *E. coli* for the *in vitro* synthesis of acyl-nucleosomes that contained an azide functionality and successfully used these recombinant acyl-nucleosomes in conjunction with the strain-promoted azide-alkyne cycloaddition reaction for acyl-nucleosome labeling to study SIRT7, an epigenetic histone modifier. Our data indicated that SIRT7 is a highly active histone H3 K36 deacylase and this activity is chromatin-dependent. We further showed that SIRT7 interactions with chromatin DNA are electrostatic in nature and SIRT7 is catalytically active to remove acetylation of H3 K36 in cells. H3K36ac natively leads to a weakened nucleosome structure that might contribute to euchromatin formation and active transcription. Our data suggest several novel non-mutually exclusive models in which removal of H3K36ac by SIRT7 in distinct settings may contribute to rDNA heterochromatin silencing and stability, active transcriptional elongation, or DNA damage repair.

Supplementary Material

Refer to Web version on PubMed Central for supplementary material.

ACKNOWLEDGMENT

We gratefully acknowledge support from National Institutes of Health (GM121584 to W.R.L., AG050997 to K.F.C., and GM086703 to H.L.), Welch Foundation (grant A-1715 to W.R.L.), and Merit Award from the Department of Veterans Affairs to K.F.C. for financial support.

REFERENCES

- (1). Brachmann CB; Sherman JM; Devine SE; Cameron EE; Pillus L; Boeke JD *Genes Dev* 1995, 9, 2888. [PubMed: 7498786]
- (2). Imai S; Armstrong CM; Kaerberlein M; Guarente L *Nature* 2000, 403, 795. [PubMed: 10693811]
- (3). North BJ; Marshall BL; Borra MT; Denu JM; Verdin E *Mol Cell* 2003, 11, 437. [PubMed: 12620231]
- (4). Jackson MD; Denu JM *J Biol Chem* 2002, 277, 18535. [PubMed: 11893743]
- (5). Denu JM *Curr Opin Chem Biol* 2005, 9, 431. [PubMed: 16122969]
- (6). Houtkooper RH; Pirinen E; Auwerx J *Nat Rev Mol Cell Biol* 2012, 13, 225. [PubMed: 22395773]
- (7). Vaquero A; Scher M; Erdjument-Bromage H; Tempst P; Serrano L; Reinberg D *Nature* 2007, 450, 440. [PubMed: 18004385]
- (8). Michishita E; McCord RA; Berber E; Kioi M; Padilla-Nash H; Damian M; Cheung P; Kusumoto R; Kawahara TLA; Barrett JC; Chang HY; Bohr VA; Ried T; Gozani O; Chua KF *Nature* 2008, 452, 492. [PubMed: 18337721]
- (9). Grob A; Roussel P; Wright JE; McStay B; Hernandez-Verdun D; Sirri V *J Cell Sci* 2009, 122, 489. [PubMed: 19174463]
- (10). Kiran S; Anwar T; Kiran M; Ramakrishna G *Cell Signal* 2015, 27, 673. [PubMed: 25435428]
- (11). Martinez-Redondo P; Santos-Barrapedro I; Vaquero A *Cancer Cell* 2012, 21, 719. [PubMed: 22698398]
- (12). Lu CT; Hsu CM; Lin PM; Lai CC; Lin HC; Yang CH; Hsiao HH; Liu YC; Lin HY; Lin SF; Yang MY *Anticancer Res* 2014, 34, 7137. [PubMed: 25503141]
- (13). Yu H; Ye W; Wu J; Meng X; Liu RY; Ying X; Zhou Y; Wang H; Pan C; Huang W *Clin Cancer Res* 2014, 20, 3434. [PubMed: 24771643]
- (14). Aljada A; Saleh AM; Alkathiri M; Shamsa HB; Al-Bawab A; Nasr A *Breast Cancer (Auckl)* 2015, 9, 3. [PubMed: 25922576]
- (15). Geng Q; Peng H; Chen F; Luo R; Li R *Int J Clin Exp Pathol* 2015, 8, 1938. [PubMed: 25973086]
- (16). Malik S; Villanova L; Tanaka S; Aonuma M; Roy N; Berber E; Pollack JR; Michishita-Kioi E; Chua KF *Sci Rep* 2015, 5, 9841. [PubMed: 25923013]
- (17). McGlynn LM; McCluney S; Jamieson NB; Thomson J; MacDonald AI; Oien K; Dickson EJ; Carter CR; McKay CJ; Shiels PG *PLoS One* 2015, 10, e0131344. [PubMed: 26121130]
- (18). Singh S; Kumar PU; Thakur S; Kiran S; Sen B; Sharma S; Rao VV; Poongothai AR; Ramakrishna G *Tumour Biol* 2015, 36, 6159. [PubMed: 25794641]
- (19). Wang HL; Lu RQ; Xie SH; Zheng H; Wen XM; Gao X; Guo L *Asian Pac J Cancer Prev* 2015, 16, 3573. [PubMed: 25921180]
- (20). Zhang S; Chen P; Huang Z; Hu X; Chen M; Hu S; Hu Y; Cai T *Sci Rep* 2015, 5, 9787. [PubMed: 25860861]
- (21). Barber MF; Michishita-Kioi E; Xi Y; Tasselli L; Kioi M; Moqtaderi Z; Tennen RI; Paredes S; Young NL; Chen K; Struhl K; Garcia BA; Gozani O; Li W; Chua KF *Nature* 2012, 487, 114. [PubMed: 22722849]
- (22). Ford E; Voit R; Liszt G; Magin C; Grummt I; Guarente L *Genes Dev* 2006, 20, 1075. [PubMed: 16618798]

- (23). Paredes S; Angulo-Ibanez M; Tasselli L; Carlson SM; Zheng W; Li TM; Chua KF *J Biol Chem* 2018.
- (24). Chen S; Seiler J; Santiago-Reichert M; Felbel K; Grummt I; Voit R *Mol Cell* 2013, 52, 303. [PubMed: 24207024]
- (25). Blank MF; Grummt I *Transcription* 2017, 8, 67. [PubMed: 28067587]
- (26). Ashraf N; Zino S; Macintyre A; Kingsmore D; Payne AP; George WD; Shiels PG *Br J Cancer* 2006, 95, 1056. [PubMed: 17003781]
- (27). De Nigris F; Cerutti J; Morelli C; Califano D; Chiariotti L; Viglietto G; Santelli G; Fusco A *Br J Cancer* 2002, 87, 1479.
- (28). Vakhrusheva O; Braeuer D; Liu Z; Braun T; Bober E *J Physiol Pharmacol* 2008, 59 Suppl 9, 201.
- (29). Vakhrusheva O; Smolka C; Gajawada P; Kostin S; Boettger T; Kubin T; Braun T; Bober E *Circ Res* 2008, 102, 703. [PubMed: 18239138]
- (30). Vazquez BN; Thackray JK; Simonet NG; Kane-Goldsmith N; Martinez-Redondo P; Nguyen T; Bunting S; Vaquero A; Tischfield JA; Serrano L *EMBO J* 2016, 35, 1488. [PubMed: 27225932]
- (31). Paredes S; Chua KF *EMBO J* 2016, 35, 1483. [PubMed: 27302089]
- (32). Tong Z; Wang M; Wang Y; Kim DD; Grenier JK; Cao J; Sadhukhan S; Hao Q; Lin H *ACS Chem Biol* 2017, 12, 300. [PubMed: 27997115]
- (33). Tong Z; Wang Y; Zhang X; Kim DD; Sadhukhan S; Hao Q; Lin H *ACS Chem Biol* 2016, 11, 742. [PubMed: 26907567]
- (34). Basu A; Rose KL; Zhang J; Beavis RC; Ueberheide B; Garcia BA; Chait B; Zhao Y; Hunt DF; Segal E; Allis CD; Hake SB *Proc Natl Acad Sci U S A* 2009, 106, 13785. [PubMed: 19666589]
- (35). Morris SA; Rao B; Garcia BA; Hake SB; Diaz RL; Shabanowitz J; Hunt DF; Allis CD; Lieb JD; Strahl BD *J Biol Chem* 2007, 282, 7632. [PubMed: 17189264]
- (36). Hsu WW; Wu B; Liu WR *ACS Chem Biol* 2016, 11, 792. [PubMed: 26820517]
- (37). Neumann H; Peak-Chew SY; Chin JW *Nat Chem Biol* 2008, 4, 232. [PubMed: 18278036]
- (38). Umehara T; Kim J; Lee S; Guo LT; Soll D; Park HS *FEBS Lett* 2012, 586, 729. [PubMed: 22289181]
- (39). Gil R; Barth S; Kanfi Y; Cohen HY *Nucleic Acids Res* 2013, 41, 8537. [PubMed: 23892288]
- (40). Feldman JL; Baeza J; Denu JM *J Biol Chem* 2013, 288, 31350. [PubMed: 24052263]
- (41). Jiang H; Khan S; Wang Y; Charron G; He B; Sebastian C; Du J; Kim R; Ge E; Mostoslavsky R; Hang HC; Hao Q; Lin H *Nature* 2013, 496, 110. [PubMed: 23552949]
- (42). Du J; Zhou Y; Su X; Yu JJ; Khan S; Jiang H; Kim J; Woo J; Kim JH; Choi BH; He B; Chen W; Zhang S; Cerione RA; Auwerx J; Hao Q; Lin H *Science* 2011, 334, 806. [PubMed: 22076378]
- (43). Mathias RA; Greco TM; Oberstein A; Budayeva HG; Chakrabarti R; Rowland EA; Kang YB; Shenk T; Cristea IM *Cell* 2014, 159, 1615. [PubMed: 25525879]
- (44). Peng C; Lu Z; Xie Z; Cheng Z; Chen Y; Tan M; Luo H; Zhang Y; He W; Yang K; Zwaans BM; Tishkoff D; Ho L; Lombard D; He TC; Dai J; Verdin E; Ye Y; Zhao Y *Mol Cell Proteomics* 2011, 10, M111.012658.
- (45). Park J; Chen Y; Tishkoff DX; Peng C; Tan M; Dai L; Xie Z; Zhang Y; Zwaans BM; Skinner ME; Lombard DB; Zhao Y *Mol Cell* 2013, 50, 919. [PubMed: 23806337]
- (46). Tan M; Peng C; Anderson KA; Chhoy P; Xie Z; Dai L; Park J; Chen Y; Huang H; Zhang Y; Ro J; Wagner GR; Green MF; Madsen AS; Schmiesing J; Peterson BS; Xu G; Ilkayeva OR; Muehlbauer MJ; Braulke T; Muhlhansen C; Backos DS; Olsen CA; McGuire PJ; Pletcher SD; Lombard DB; Hirschey MD; Zhao Y *Cell Metab* 2014, 19, 605. [PubMed: 24703693]
- (47). Li L; Shi L; Yang S; Yan R; Zhang D; Yang J; He L; Li W; Yi X; Sun L; Liang J; Cheng Z; Shi L; Shang Y; Yu W *Nat Commun* 2016, 7, 12235. [PubMed: 27436229]
- (48). Wang WW; Zeng Y; Wu B; Deiters A; Liu WR *ACS Chem Biol* 2016, 11, 1973. [PubMed: 27152839]
- (49). Lee YJ; Kurra Y; Yang Y; Torres-Kolbus J; Deiters A; Liu WR *Chem Commun (Camb)* 2014, 50, 13085. [PubMed: 25224663]
- (50). Debets MF; van Berkel SS; Schoffelen S; Rutjes FP; van Hest JC; van Delft FL *Chem Commun* 2010, 46, 97.

- (51). Baskin JM; Prescher JA; Laughlin ST; Agard NJ; Chang PV; Miller IA; Lo A; Codelli JA; Bertozzi CR Proc Natl Acad Sci U S A 2007, 104, 16793. [PubMed: 17942682]
- (52). Gordon CG; Mackey JL; Jewett JC; Sletten EM; Houk KN; Bertozzi CR J Am Chem Soc 2012, 134, 9199. [PubMed: 22553995]
- (53). Luger K; Rechsteiner TJ; Richmond TJ Methods Mol Biol 1999, 119, 1. [PubMed: 10804500]
- (54). Eymery A; Horard B; El Atifi-Borel M; Fourel G; Berger F; Vitte AL; Van den Broeck A; Brambilla E; Fournier A; Callanan M; Gazzeri S; Khochbin S; Rousseaux S; Gilson E; Voure'h C Nucleic Acids Res 2009, 37, 6340. [PubMed: 19720732]
- (55). Luger K; Mader AW; Richmond RK; Sargent DF; Richmond TJ Nature 1997, 389, 251. [PubMed: 9305837]
- (56). Wang Z; Zang C; Rosenfeld JA; Schones DE; Barski A; Cuddapah S; Cui K; Roh TY; Peng W; Zhang MQ; Zhao K Nat Genet 2008, 40, 897. [PubMed: 18552846]
- (57). Kim H; Jo H; Seo HD; Park HS; Lee D Biochem Biophys Res Commun 2018, 503, 1200. [PubMed: 30005873]
- (58). Neumann H; Hancock SM; Buning R; Routh A; Chapman L; Somers J; Owen-Hughes T; van Noort J; Rhodes D; Chin JW Mol Cell 2009, 36, 153. [PubMed: 19818718]
- (59). Tanabe K; Liu J; Kato D; Kurumizaka H; Yamatsugu K; Kanai M; Kawashima SA Sci Rep 2018, 8, 2656. [PubMed: 29422688]
- (60). Aramsangtienchai P; Spiegelman NA; He B; Miller SP; Dai L; Zhao Y; Lin H ACS Chem Biol 2016, 11, 2685. [PubMed: 27459069]
- (61). Kutil Z; Novakova Z; Meleshin M; Mikesova J; Schutkowski M; Barinka C ACS Chem Biol 2018, 13, 685. [PubMed: 29336543]
- (62). Schultz BE; Misialek S; Wu J; Tang J; Conn MT; Tahilramani R; Wong L Biochemistry 2004, 43, 11083. [PubMed: 15323567]
- (63). Wu M; Hayward D; Kalin JH; Song Y; Schwabe JW; Cole PA Elife 2018, 7:e37231. [PubMed: 29869982]
- (64). Mahrez W; Arellano MS; Moreno-Romero J; Nakamura M; Shu H; Nanni P; Kohler C; Gruissem W; Hennig L Plant Physiol 2016, 170, 1566. [PubMed: 26764380]
- (65). Scholz C; Weinert BT; Wagner SA; Beli P; Miyake Y; Qi J; Jensen LJ; Streicher W; McCarthy AR; Westwood NJ; Lain S; Cox J; Matthias P; Mann M; Bradner JE; Choudhary C Nat Biotechnol 2015, 33, 415. [PubMed: 25751058]

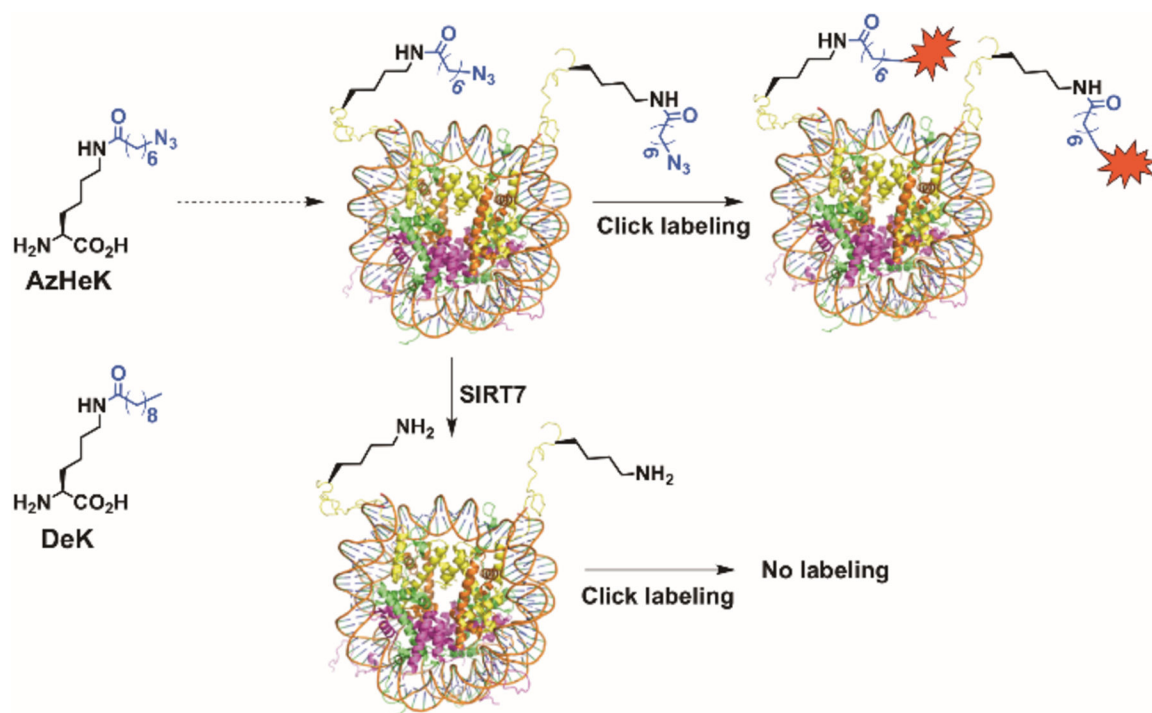


Figure 1.

A click chemistry-based approach to profile SIRT7-targeted chromatin lysine deacylation sites. AzHeK that structurally resembles DeK is site-specifically incorporated into a histone that is further assembled *in vitro* with other histones and 601 DNA into an acyl-nucleosome. This acyl-nucleosome can be labeled fluorescently with a strained alkyne dye and subsequently visualized in a 1× TBE native-PAGE gel. When SIRT7 is catalytically active to remove fatty acylation from the incorporated AzHeK to recover lysine, incubating the assembled acyl-nucleosome with SIRT7 will remove the fatty acylation and therefore afford a deacylated nucleosome that cannot be labeled fluorescently and then visualized in a gel.

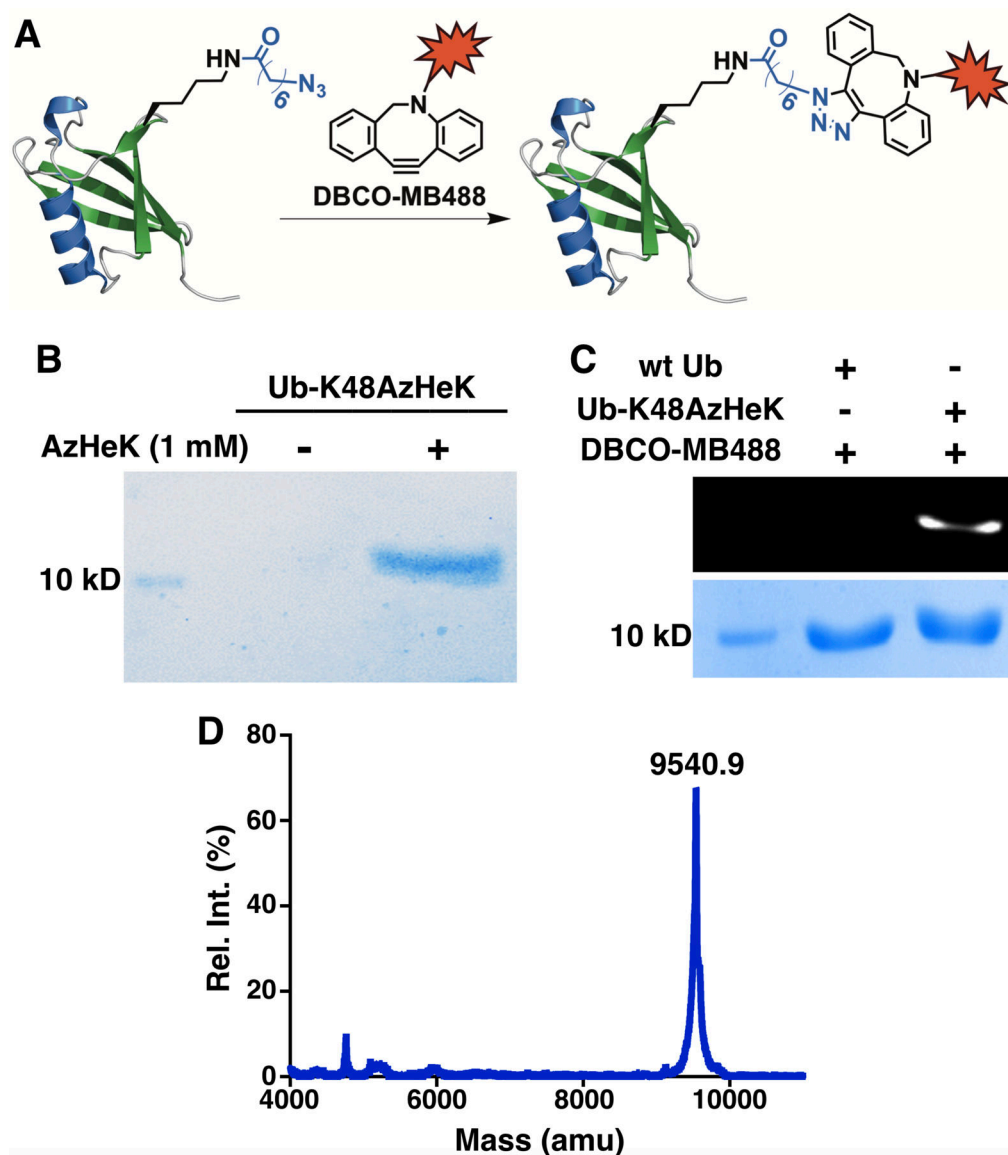


Figure 2.

The genetic incorporation of AzHeK. **(A)** A diagram to illustrate the fluorescent labeling of a genetically incorporated AzHeK in a protein with MB488-DBCO, a strained alkyne dye from Click Chemistry Tools LLC. **(B)** The selective incorporation of AzHeK into ubiquitin at its K48 position to afford UbK48az. We transformed BL21(DE3) cells with plasmid pEVOL-OcKRS coding OcKRS and tRNA^{Py1}_{CUA} and plasmid pETDuet-UbK48Am coding a ubiquitin gene with an amber mutation at the K48 coding position and then grew the transformed cells in 2YT media with or without 1 mM AzHeK. **(C)** The selective labeling of UbK48az with MB488-DBCO. Reaction conditions: we incubated UbK48az with 100 μ M DBCO-MB488 for 1 h before doing the in-gel fluorescence analysis. **(D)** The MALDI-TOF MS spectrum of UbK48az. The calculated molecular weight is 9540.7 Da.

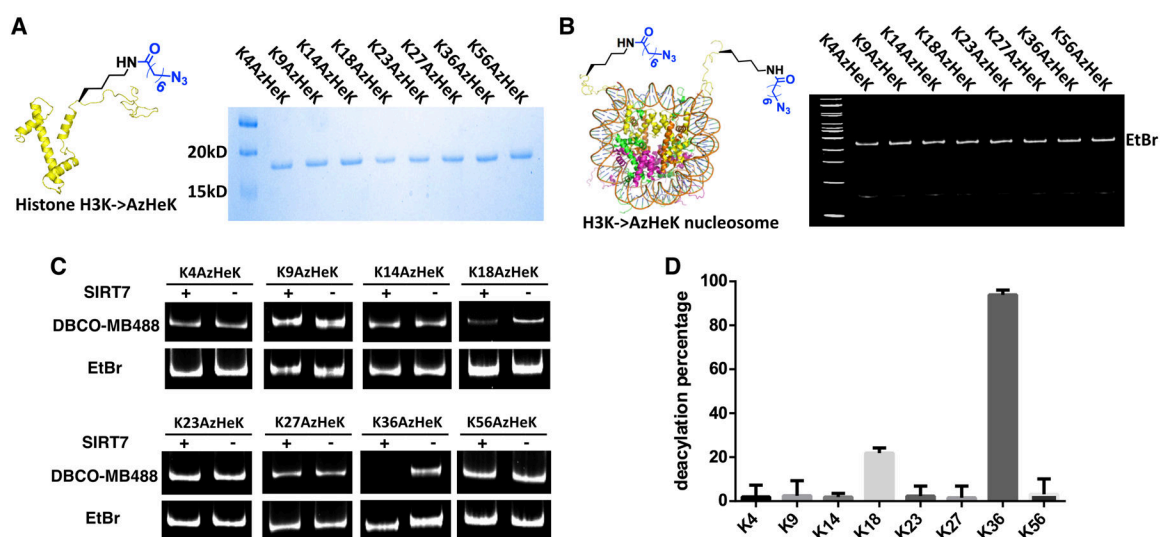


Figure 3. SIRT7 actively removes acylation from H3 K18 and H3 K36 in the nucleosome context. **(A)** SDS-PAGE analysis of eight purified AzHeK-containing H3 proteins. **(B)** Acyl-nucleosomes that we assembled from eight acyl-H3 proteins, H2A, H2B, H4, and 601 DNA (147 bp). Nu-H3K4az denotes an acyl-nucleosome assembled from H3K4az. All other acyl-nucleosomes are named in the same way. Mononucleosomes are typically shown around the 500 bp DNA position in an EtBr-stained 5% 1 \times TBE native-PAGE gel. **(C)** SIRT7 catalyzed deacylation activities on eight acyl-nucleosome substrates. Reaction conditions: we incubated 1 μ M acyl-nucleosome with 0.5 μ M SIRT7, 0.5 mM BME and 1 mM NAD⁺ at 37 °C for 2 h before we quenched the reaction by the addition of 20 mM nicotinamide. We then labeled the resulted acyl-nucleosome substrate with 100 μ M MB488-DBCO for 1 h and analyzed it fluorescently in an 8% 1 \times TBE native-PAGE gel. The top panel shows the MB488-DBCO-based fluorescent imaging and the bottom panel shows the EtBr-stained DNA from the same gel. **(D)** Quantified deacylation levels at eight H3 lysine sites. We repeated experiments show in **C** thrice and calculated the deacylation level at each site by subtracting average MB488-DBCO-based fluorescence intensity of SIRT7-treated samples from that of untreated controls.

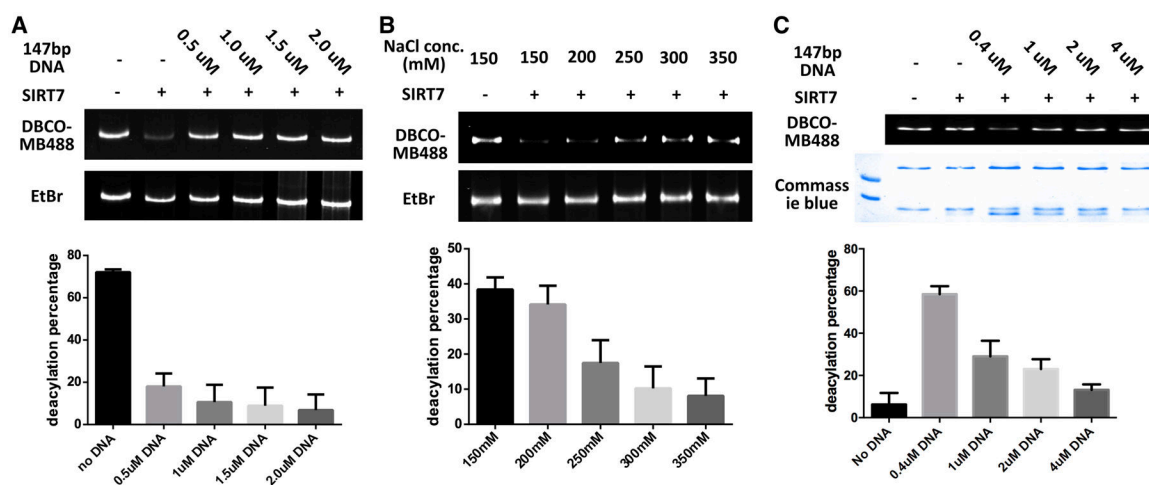


Figure 4.

Effects of DNA and salt on SIRT7-catalyzed deacylation. **(A)** Free DNA inhibits SIRT7-catalyzed nucleosome deacylation. Reaction conditions: we incubated 1 μM nu-H3K36az with 0.1 μM SIRT7, a varied concentration of 147 bp DNA, 1 mM NAD^+ and 0.5 mM BME at 37 $^{\circ}\text{C}$ for 3 h before we labeled the solution with 100 μM MB488-DBCO and analyzed the acyl-nucleosome substrate fluorescently in a $1\times$ TBE native-PAGE gel. The top panel is MB488-DBCO-based imaging that indicates relative acylation levels and the bottom panel is EtBr-based imaging that confirms the nucleosome integrity. **(B)** Salt inhibits SIRT7-catalyzed nucleosome deacylation. Conditions were as same as in **A** except we replaced free DNA with NaCl. **(C)** Free DNA has a binary role on SIRT7-catalyzed deacylation of the H3K36az-H4 tetramer substrate. Reaction conditions: we incubated 2 μM H3K36az-H4 tetramer with 1 μM SIRT7, a varied concentration of 147 bp DNA, 0.5 mM BME, and 1 mM NAD^+ at 37 $^{\circ}\text{C}$ for 2 h before we labeled the solution with 100 μM MB488-DBCO and analyzed the tetramer substrate fluorescently in a SDS-PAGE gel.

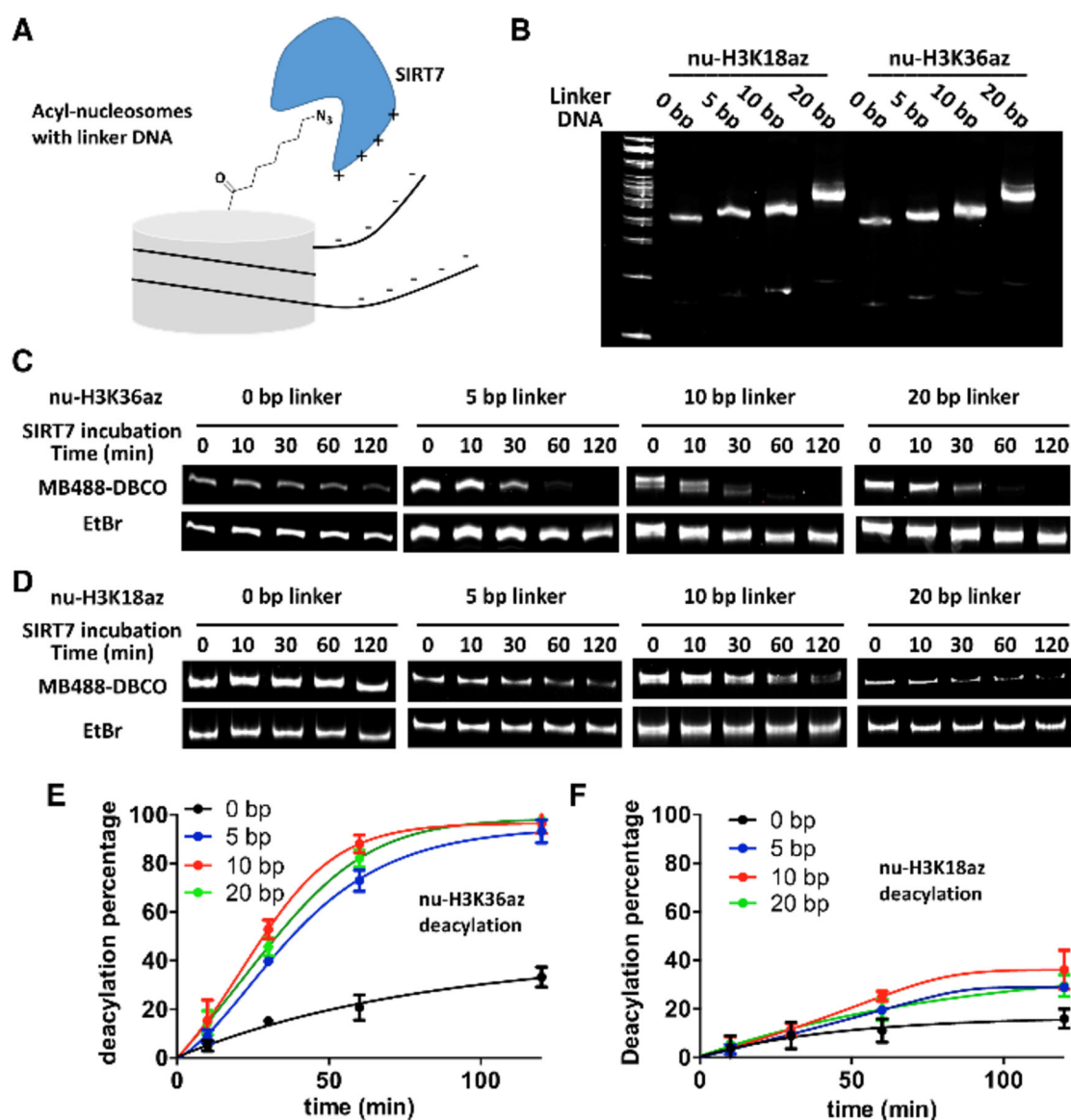


Figure 5.

A linker DNA on an acyl-nucleosome substrate improves SIRT7-catalyzed deacylation. (**A**) A diagram to illustrate how a linker DNA facilitates the binding of SIRT7 to an acyl-nucleosome substrate. (**B**) The *in vitro* assembly of nu-H3K18az and nu-H3K36az with different lengths of linker DNAs. The gel showed the EtBr-stained nucleosomes. (**C**) The catalytic removal of acylation from nu-H3K36az substrates that contained different lengths of linker DNAs. Reaction conditions: we incubated a 1 μ M H3K36az nucleosome with 0.1 μ M SIRT7, 1 mM NAD⁺ and 0.5 mM BME at 37 °C for various times before we quenched the reaction by adding 20 mM nicotinamide, labeled the solution with 100 μ M MB488-DBCO for 1 h, and then analyzed the nucleosome substrate fluorescently by 8% 1 \times TBE native-PAGE gel. (**D**) The catalytic removal of acylation from nu-H3K18az substrates that contained different lengths of linker DNAs. Reaction conditions were as same as for nu-H3K36az substrates except higher amount of SIRT7 (0.3 μ M) was used. (**E-F**) Quantified

deacylation percentage vs time for two acyl-nucleosome substrates. Reactions shown in **C** and **D** were repeated thrice. Deacylation was calculated and averaged by subtracting MB488-DBCO-based fluorescence intensity at different time points from that at 0 min.

Author Manuscript

Author Manuscript

Author Manuscript

Author Manuscript

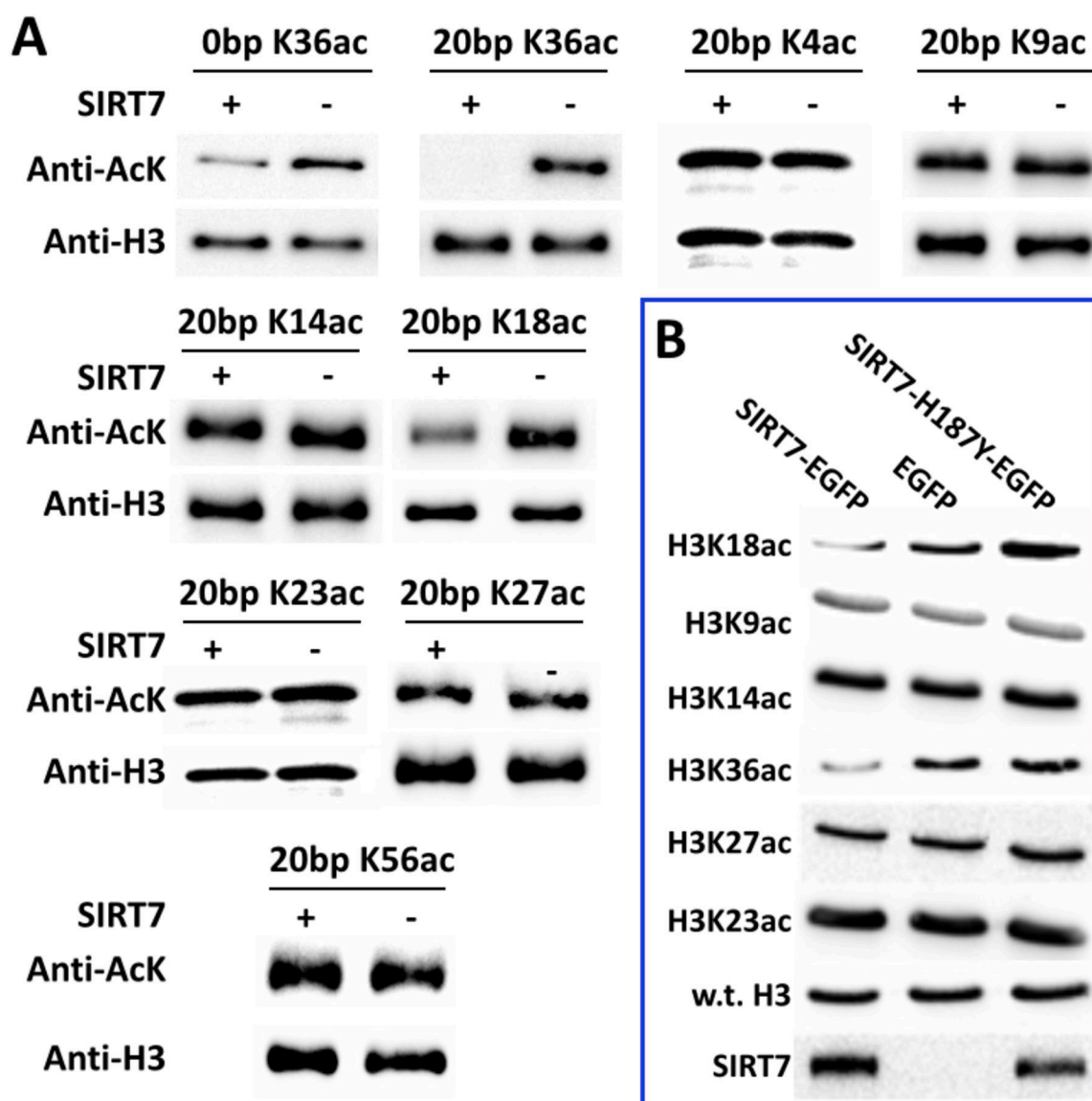


Figure 6.

SIRT7 catalyzes deacetylation at H3 K18 and H3 K36 in cells. **(A)** SIRT7 activities on a number of *in vitro* assembled acetyl-nucleosomes. Reaction conditions: we incubated an acetyl-nucleosome (1 μ M) with or without 0.3 μ M SIRT7 for 2 h before we analyzed the reaction by SDS-PAGE and then probed the acetylation level and H3 by anti-H3K36ac antibody and an anti-H3 antibody, respectively. We tested both a nu-H3K36ac nucleosome without a linker DNA and the one with a 20 bp linker DNA. All other acetyl-nucleosomes contained a 20 bp linker DNA. **(B)** Acetylation levels detected by Western blotting at K9, K14, K18, K23, K27, and K36 of histone H3 in SIRT7-transfected cells with respect to those in control cells that expressed just EGFP or an inactive SIRT7 mutant. Signals were probed by site-specific Kac antibodies.

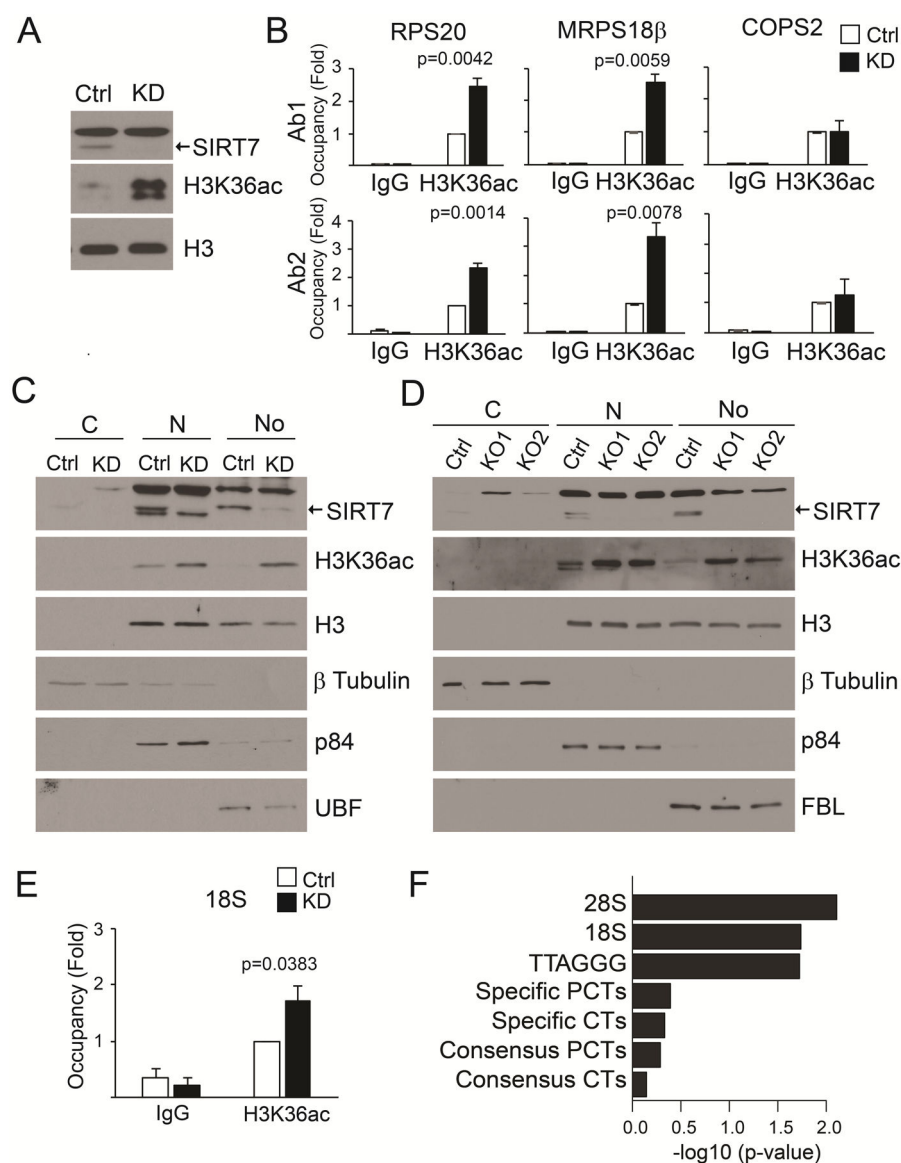


Figure 7. SIRT7 is a physiologic nucleolar and nucleoplasmic H3K36 deacetylase. **(A)** Immunoblot showing increased H3K36ac levels in whole cell lysates from SIRT7 knock-down (KD) U2OS cells compared to control cells. **(B)** ChIP-PCR showing increased H3K36ac levels at promoters of SIRT7 target genes RPS20 and MRPS18b, but not COPS2, in SIRT7 KD versus control U2OS cells. Two independent H3K36ac antibodies (Ab 1 and 2) were used. Data show the average of three technical replicates \pm SEM, and are representative of 2–4 biological replicates. Statistical significance was calculated performing Student’s t-test. **(C)** Immunoblot of nucleolar fractionation showing increased levels of H3K36ac in SIRT7 KD cells versus control cells. β -Tubulin, p84, and FBL or UBF are shown as marker controls for cytoplasmic, nucleoplasmic, and nucleolar fractions, respectively. **(D)** Immunoblot of nucleolar fractionation of SIRT7 knockout versus control U2OS cells. **(E)** ChIP-PCR showing increased levels of H3K36ac at 18S rDNA sequences in SIRT7 KD cells. Data

show the average of three biological replicates \pm SEM. Statistical significance was calculated performing Student's t-test. (F) ChIP-seq enrichment analysis of H3K36ac at repetitive sequences in SIRT7 KD versus control U2OS cells. Bar plot of \log_{10} (p-value) shows statistically significant enrichment of H3K36ac in SIRT7-KD cells at rDNA (18S, 28S) and telomeric (TTAGGG) repeats, but not at repetitive sequences from 20 specific centromeres (CT), 6 specific pericentromeres (PCT), or 4 centromeric and 4 pericentric consensus sequences. P-values were calculated performing Chi-squared test.

Author Manuscript

Author Manuscript

Author Manuscript

Author Manuscript

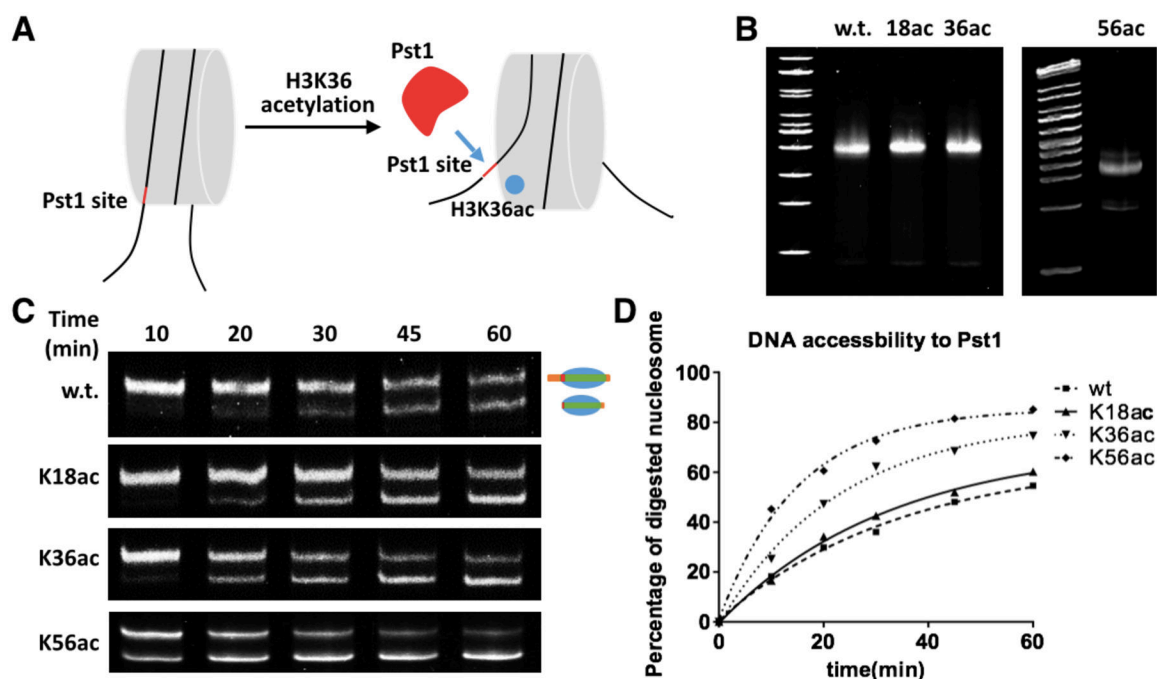


Figure 8.

Lysine acetylation at H3 K36 improves DNA unwrapping from the nucleosome core. (A) A diagram to illustrate how H3K36ac increases DNA unwrapping from the nucleosome core and subsequent Pst1 access to an embedded Pst1 restriction site. (B) The *in vitro* assembly of three nucleosomes, nu', nu'-H3K18ac, nu'-H3K36ac, and nu'-H3K56ac from corresponding histones and a mutant 601 DNA that had a Pst1 restriction site and a linker DNA. The gel shows EtBr-stained nucleosomes. (C) Pst1 digestion progress of four nucleosomes versus time. Reaction conditions: we incubated a 0.49 μ M nucleosome with 2 U/uL Pst1 at 37 °C for various times before the reaction was stopped and the solution was analyzed by 5% 1 \times TBE native-PAGE. The gel was stained by EtBr. The top band in a lane shows the nucleosome with the linker DNA and the bottom band represents the one with the linker DNA removed. (D) The calculated ratio of digested nucleosome to undigested nucleosome vs time. We calculated and averaged the ratios based on integrated fluorescence intensities of original and digested nucleosome bands in gels.

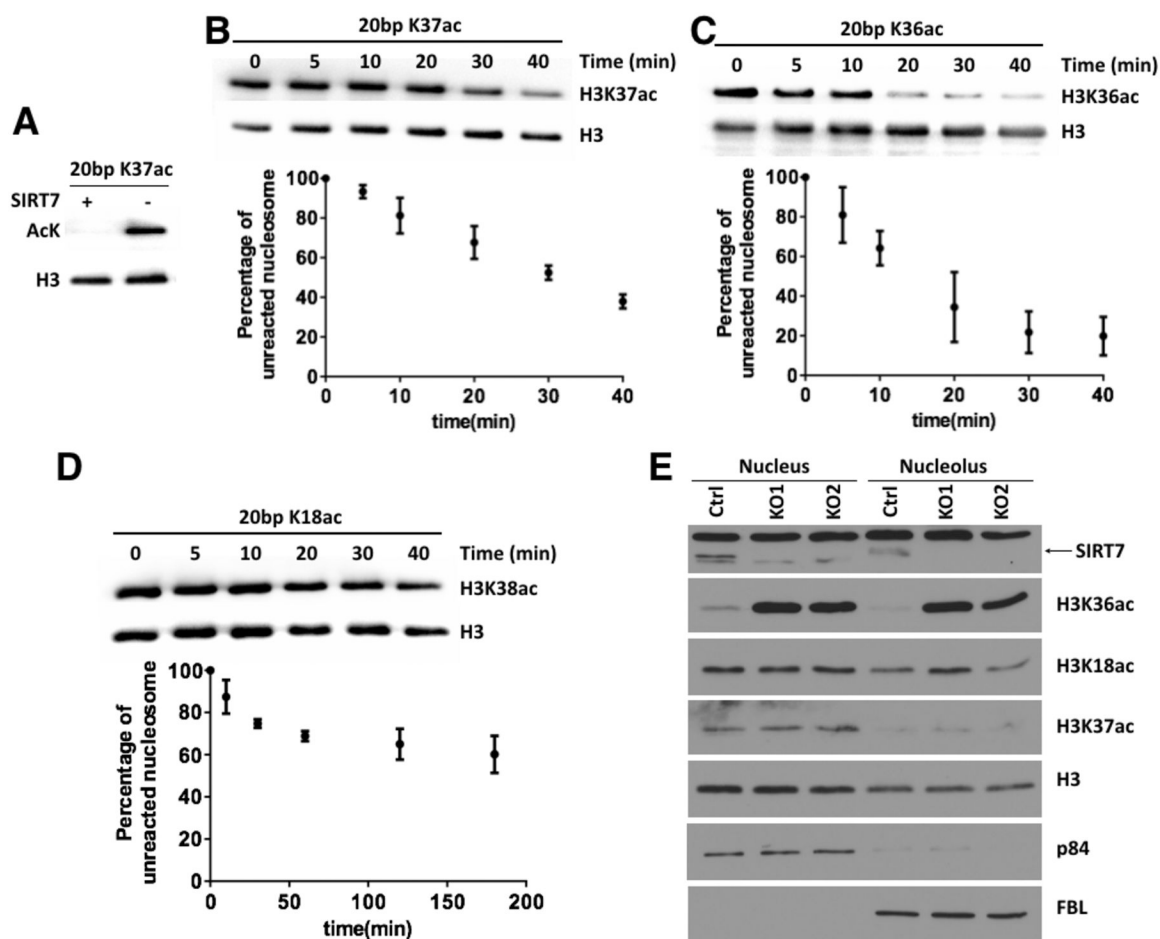


Figure 9.

SIRT7 deacetylates H3K37ac *in vitro*. (A) *In vitro* deacetylation of nu-H3K37ac by SIRT7. Reaction conditions: nu-H3K37ac (1 μ M) was incubated with or without 0.3 μ M SIRT7 for 2 h, and then analyzed by SDS-PAGE and Western blot. (B-D) Time-based deacetylation of nu-H3K37ac, nu-H3K36ac, and nu-H3K18ac by SIRT7. Reaction conditions: 1 μ M acetyl-nucleosomes were incubated with 0.1 μ M SIRT7, 1 mM NAD⁺ and 0.5 mM BME at 37 °C for various times followed by reaction quenching in 20 mM nicotinamide, and acetylation levels were analyzed by Western blot. Reactions were repeated thrice and average acetylation levels at different times are presented in the bottom panel diagram. (E) Immunoblot of nucleoplasmic and nucleolar fractions from control and SIRT7 knockout cell lines. Data showed global increase in H3K36ac but not H3K18ac or H3K37ac levels. p84 and FBL are shown as marker controls for nucleoplasmic and nucleolar fractions, respectively.